Available online at www.sciencedirect.com

ScienceDirect

Energy Procedia 66 (2015) 77 – 80

Energy Procedia

The 12th International Conference on Combustion & Energy Utilisation – 12ICCEU

The Effect of Ethanol Blending on Combustion and Soot Formation in an Optical DISI Engine Using High-Speed Imaging

M. Storch, S. Erdenkäufer, M. Wensing, S. Will, L. Zigan*

Lehrstuhl für Technische Thermodynamik (LTT) and Erlangen Graduate School in Advanced Optical Technologies (SAOT), Friedrich-Alexander-Universität Erlangen-Nürnberg (FAU), Germany

Abstract

Biofuel components exhibit significantly different fuel properties as compared to gasoline leading to a very complex chain of effects in engine combustion. Therefore, the effects of varying composition on mixture formation, combustion and soot formation can hardly be predicted. In this study, the influence of blending 20vol% ethanol to isooctane is investigated by simultaneous OH*-chemiluminescence and soot radiation high-speed imaging. For both fuels engine load was varied for a typical catalyst heating operating point, which is characterized by increased soot formation probability. The study reveals an unexpected behavior for E20. Both the OH*-chemiluminescence and soot luminosity intensity are higher as compared to isooctane. Furthermore, for E20 the occurrence probability of droplet combustion is increased. High engine load increases the combustion intensities and probability of soot formation for both investigated fuels.

Peer-review under responsibility of the Engineering Department, Lancaster University

Keywords: DISI engine, Isooctane/ethanol blends, OH*-chemiluminescence,soot radiation

1. Introduction

Sources of soot formation in direct injection spark ignition (DISI) engines are manifold. Among others, in stratified operation mode, locally fuel rich mixture zones and incompletely vaporized liquid fuel droplets are significant for soot formation [1]. This soot formation mechanism is important for the catalyst heating operation mode, which is characterized by spark retard strategy and late injection in order to heat up the exhaust gas system for proper three-way-catalyst operation [2]. Besides this, there are fuel specific effects which may have an important impact on particulate matter (PM) emission, especially when blending with ethanol [3].

In general, ethanol blended fuels show reduced PM emissions in comparison to gasoline and its surrogate fuels [4]. However, there are also studies reporting increasing particulate concentration for gasoline engine fuels with higher ethanol content [5]. Maricq et al. found [6] that with ethanol contents in gasoline

* Lars Zigan. Tel.: +49-9131-85 29770
E-mail address: Lars.Zigan@cbi.uni-erlangen.de

Peer-review under responsibility of the Engineering Department, Lancaster University
doi:10.1016/j.egypro.2015.02.041

below 20 vol% there is a small benefit for particulate number emission reduction. A significant decrease in PM exhaust emission was measured for higher ethanol contents (> 30 vol%). Karavalkis et al. obtained similar results for fuels with low ethanol content. Here blends with intermediate ethanol content (E15, E20) not necessarily showed PM mass reductions, although the fuel oxygen content was increased [7]. Possible reasons for these results could be the non-ideal mixing behavior of ethanol blended fuels, which were found in evaporating single droplets [8]. Furthermore, the ethanol specific high in-cylinder cooling could affect the fuel evaporation and mixing process [3].
In this study, the combustion and sooting behavior of isooctane and the mixture E20 (20 vol% of ethanol in isooctane) is analyzed in an optical accessible DISI engine. Purposely a sooting operating point (catalyst heating) was produced where the effect of the fuel on sooting behavior can be studied by simultaneous high speed imaging of OH*-chemiluminescence and natural soot luminosity.

2. Experimental Setup

The measurements in the present work were performed in a modern single cylinder optical engine based on a series-production direct injection engine with four valves per cylinder and a variable valve train.
Isooctane was used as surrogate fuel for gasoline. It is compared to a mixture of 20 vol% of ethanol in isooctane (E20). As operating condition a part load catalyst heating operating point was chosen. It is characterized by multiple, late injection and late ignition, which increases the probability of soot formation (see Table 1). OP1 is similar to OP2, characterized by a higher load. It is assumed that high ambient pressure negatively affects the evaporation of the fuel spray for the second injection event which is at 73 °CA BTDC. The difference in heating values between the two fuels was adjusted by injection duration.
For the optical setup, a Phantom v711 high-speed CMOS camera in combination with an image intensifier and an image stereoscope was used. The camera was driven at a frequency of 7200 Hz, which corresponds to one image per °CA at 1200 rpm. The image stereoscope contained a 308 ±25 nm and a 568 ±10 nm bandpass filter in order to detect OH*-chemiluminescence and black body radiation simultaneously.

Table 1. Operating points with characteristic engine parameters.

Operating Point	Engine Speed (rpm)	Air Mass Flow (kg/h)	Global Lambda (-)	Engine Load (bar) Isooctane / E20		Rail Pressure (bar)	SOI1/SOI2 (°CA BTDC)	Inj. Duration (ms) Isooctane / E20		Spark Timing (°CA BTDC)
OP1	1200	4.8	1	1.8	1.7	70	300/73	0.94/0.25	0.96/0.25	0
OP2	1200	6.5	1	3.0	3.2	70	300/73	1.25/0.25	1.28/0.25	0

3. Results

In Figure 1, exemplarily selected images of a typical engine cycle are displayed for isooctane and E20 for OP1 and OP2 in both wavelength regions. Three different time steps are presented in °CA after top dead center (aTDC). In general, the OH*-chemiluminescence channel shows initial flame propagation. The soot luminosity channel always shows lower signal intensities than the chemiluminescence channel, but occasionally single bright spots can be detected. It is assumed that these bright structures are caused by diffusion flame combustion of not fully evaporated fuel droplets, which remain from the late injection process of the second injection event. Here, strong soot formation is expected. These structures in general appear in the middle of the cylinder near the spark plug. At low engine load (OP1) the chemiluminescence of the two fuels does not significantly differ whereas the soot luminosity is more intense for E20 in comparison to isooctane. For E20 the chemiluminescence signal is located at the same region as the soot luminosity in the combustion chamber. This means that visible soot in that area is still

being oxidized. At high engine load (OP2) the combustion of both fuels is more advanced at the same point of time in comparison to low engine load although the injection and ignition time points are the same.

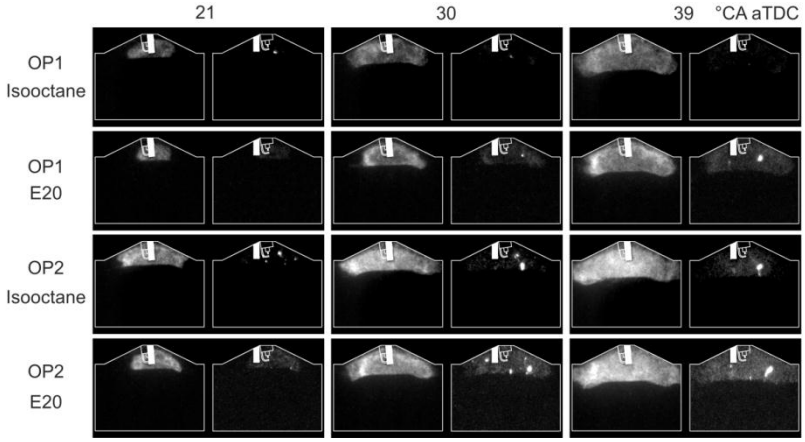

Figure 1. High-speed resolved single combustion cycle for isooctane and E20 for OP1 and OP2. The images are termed in °CA after Top Dead Center. The spark plug is marked in the top-middle of the image. The left half image shows OH*-chemiluminescence and the right half image shows soot luminosity.

At high engine load (OP2) the combustion of both fuels is more advanced at the same point of time in comparison to low engine load, although the injection and ignition time point is the same. Furthermore, the intensities are stronger for both chemiluminescence and soot luminosity. This is due to larger fuel mass at constant air-fuel ratio at increased engine load. Also the occurrence frequency and intensity of droplet combustion are increased at higher load for both fuels. This is due to the reduced evaporation rate at high combustion chamber pressure.

In order to quantify the results, the images are averaged and single channels are considered separately. The OH*-chemiluminescence channel is termed combustion mode M#1, which is also an indicator for heat release rate. The soot luminosity channel is termed combustion mode M#2, which corresponds mainly to homogenously distributed soot radiation in the images. In addition, also the bright intensity structures (droplet combustion) are considered separately and are further on termed combustion mode M#3. In the following, all three combustion modes are compared, averaged over 30 cycles and presented temporally resolved for the two fuels and operating points in Fig. 2.

For combustion mode M#1 (left) it can be seen that the combustion of E20 is more intense than that of isooctane, which corresponds to a higher heat release rate. E20 must have an positive effect on heat release rate and combustion efficiency as already investigated by Al-Hasan [9]. In his study E20 showed the best result regarding engine performance and the reduction of CO and HC emissions. It was assumed that E20 represents an optimum for volumetric efficiency. Considering maximum intensities, the same behavior between the two fuels can be seen at higher engine load (OP2). However, it is clear that the maximum intensity is shifted to earlier points in time for OP2 for both fuels. This is due to higher combustion chamber temperatures during compression or local rich fuel-air mixtures which enhance initial flame kernel development [1].

The difference in maximum M#2 intensity is more significant for OP2 than for OP1. Soot luminosity and the amount of generated soot may increase in comparison to low engine load because more fuel mass is burned and higher combustion temperatures are reached. Furthermore, the figure shows no significant time shift between M#1 and M#2 intensity for all fuels and operating points. In Figure 2 (right) the averaged intensity of combustion mode M#3 is displayed over °CA after TDC for both fuels and both

operating points. In comparing the curves of M#3 to M#2 they appear less smooth because of high cyclic variability.

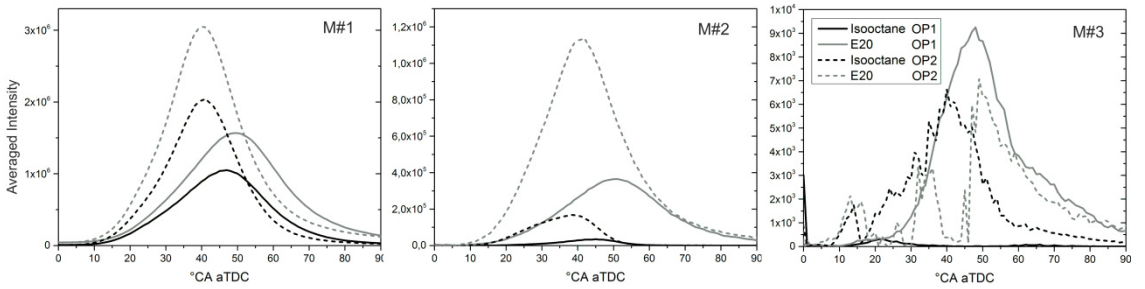

Figure 2. Averaged intensity of the combustion modes comparing OP1 and OP2 for isooctane and E20.

At low load (OP1) isooctane shows lower intensities than E20, which shows the highest maximum intensity also compared to OP2. Yet the maxima are shifted in time, the maximum intensity for isooctane apears early in the cycle (at 22°CA aTDC). Because of the temporal shift and the strong signal intensity, it is assumed that for OP1 the soot exhaust emission of E20 is increased as compared to isooctane. The reason may be incompletely evaporated fuel which can not be fully oxidized during the expansion stroke. Here, the non-ideal evaporation of ethanol in isooctane and/or the high enthalpy of evaporation of ethanol may be the underlying reason. For 20vol% of ethanol in isooctane it is assumed that the oxygen content in the fuel is too low to affect the combustion positively regarding soot formation. At higher load (OP2) these effects may be enhanced. The figure shows that the maximum intensities of isooctane and E20 are similiar. It is apparent that the intensity increases earlier than for OP1. In this case, E20 soot radiation is visible at higher level for a longer times than isooctane soot radiation, which may affect the exhaust particulate emission.

4. Conclusions

The study of simultaneous OH*-chemiluminescence and soot luminescence imaging of E20 and isooctane in an optical accessible DISI engine at catalyst heating operation lead to the following conclusions:

- E20 showed stronger OH*-chemiluminescence and soot luminosity than isooctane.
- The investigation of bright combustion structures (diffusion controlled flame for incomplete evaporated fuel droplets – M#3) revealed higher intensities for E20 in comparison to isooctane. It was found that those structures also appear longer in the cycle for E20. This may be an important source for exhaust particulate matter emission.
- An elevation in engine load increases combustion intensities and the probability of diffusion controlled droplet combustion for both fuels.

In further work particulate matter concentration is measured at the engine exhaust by LII (laser-induced incandescence). In addition, the study is extended to other fuels (E85, pure ethanol).

References

[1.] F. Zhao, M.-C. Lai, D. Harrington, Progress in Energy and Combustion Science 25, pp. 437–562 5 (1999).
[2.] W. Piock, G. Hoffmann et al., SAE International Journal of Engines 4, pp. 1455–1468 (2011).
[3.] L. Chen, R. Stone, Energy Fuels 25, pp. 1254–1259 3 (2011).
[4.] J. M. E. Storey, T. L. Barone et al., SAE Technical Paper 2012-01-0437 (2012).
[5.] R. Daniel, H. Xu et al., Applied Energy 105, pp. 252–261 (2013).
[6.] M. M. Maricq, J. J. Szente, K. Jahr, Aerosol Science and Technology 46, pp. 576–583 5 (2012).
[7.] G. Karavalakis, D. Short et al., Fuel 128, pp. 410–421 (2014).
[8.] A. Bader, P. Keller, C. Hasse, International Journal of Heat and Mass Transfer 64, pp. 547–558 (2013).
[9.] M. Al-Hasan, Energy Conversion and Management 44, pp. 1547–1561 9 (2003).